Neural, Parallel, and Scientific Computations 22 (2014) 45-58

APPROXIMATION OF ADVECTION-DIFFUSION PHENOMENON WITH WAVELETS

S. DHAWAN[1], S. ARORA[2], AND S. KUMAR[3]

[1,3] Department of Mathematics
Dr B. R. Ambedkar National Institute of Technology Jalandhar-144011, India
[2]H. M. V. College Jalandhar

ABSTRACT. There are many situations when both advection and diffusion terms are important and a transport equation needs to be solved as a whole. In the recent past, it has drawn significant attention of civil engineers, hydrologists, mathematical modelers and many others in different branches. Nowadays, wavelet approach has become very popular in the field of numerical approximations. Fascinated by their ability to accurately represent fairly general functions with a small number of adaptively chosen wavelet coefficients, we apply haar wavelet collocation scheme for the numerical simulation of advection-diffusion equation. Some test examples are studied to evaluate the performance of the solution scheme.

Keywords: Advection, diffusion, wavelets, approximation

1. Introduction

In mathematical literature, wavelet analysis was developed in 1980's and began to be used commonly in geophysics in the 1990's. In 1982 Jean Morlet a French geophysicist, introduced the concept of a 'wavelet'. The wavelet means small wave and the study of wavelet transform is a new tool for seismic signal analysis. Wavelet analysis was originally introduced in order to improve seismic signal analysis by switching from shortime Fourier analysis to new better algorithms to detect and analyze abrupt changes in signals [1, 2]. Daubechies in 1988 presented a method to construct wavelets with compact support and scale functions [3]. With the advancements in new computational schemes, wavelets contributed a lot. With some specific features, family of wavelets include different classes of wavelets as Haar, Franklin, Stetson hat, Daubechies, Coiflets, Symlets, Meyer, DMeyer, Gaussian, Morlet, Complex Gaussian, Mexican Hat etc. In general, Haar, Daubechies, Symlets and Coiflets are compactly supported orthogonal wavelets. With a solid historical as well as practical background, Haar wavelets are easy to handle from the mathematical aspect. Haar functions have been used from 1910 when they were introduced by the Hungarian

Received January 24, 2014

mathematician Alfred Haar [4]. Having properties to provide a local analysis of signals, the Haar functions appear very attractive in many applications as for example, image coding, edge extraction and binary logic design. In the present study, we use Haar wavelet method for solving the advection-diffusion equation model with given initial and boundary conditions.

In 1980s Professor T. J. R. Hughes made an extraordinary effort at Stanford and presented several interesting facts about advection-diffusion equation [5, 6]. It governs several important phenomena in physics and engineering such as water transfer in soils, the intrusion of salt water into fresh water aquifers, the spread of pollutants in rivers and streams, the intrusion of salt water into fresh water aquifers etc. (see e.g., [7, 8]). There are many situations when both advection and diffusion terms are important and a transport equation needs to be solved as a whole. Advection-diffusion equation also helps in studying the more advanced Navier-Stokes equations [9, 10]. These equations are characterized by non-dissipative (hyperbolic) advective transport component and a dissipative (parabolic) diffusive component. All numerical profiles go well when diffusion is the dominant factor. On the contrary, when advection is dominant transport process, most numerical results exhibit some combination of spurious oscillations and excessive numerical diffusion. These behaviours can be easily explained using a general Fourier analysis.

Most existing analytical solutions for advection-diffusion transport problems in [11, 12], including problems with growth and decay terms, are for semi-infinite or infinite regions, with solutions for finite domains being mostly limited to one-dimensional problems. Fascinated by the importance of advection-diffusion equation and important properties of wavelets [13, 14], we focus on a developing numerical scheme for the simulation of advection-diffusion model problem

$$\frac{\partial u}{\partial t} + \rho \frac{\partial u}{\partial x} = \varepsilon \frac{\partial^2 u}{\partial x^2}, \ (x,t) \in [0,L] \times [0,T], \tag{1.1}$$

with the given initial and boundary conditions $u(x,0) = f(x),\ u(0,t) = g_0(t),\ u(L,t) = g_1(t),\ t \in [0,T]$, with the help of wavelets. Here, $\rho, \varepsilon > 0$ are positive constants representing advection and diffusion processes respectively. We see that for $\rho = 0$, it represents purely diffusion phenomenon. Some other useful readings are [15].

2. **Construction of Haar wavelets**

Haar wavelet is one of the oldest and simplest wavelet. Therefore, any discussion of wavelets starts with the Haar wavelet. Due to the simplicity the Haar wavelets are very effective for solving ordinary differential and differential equations. Some definitions and properties of Haar functions are as [16]:

Definition 1. Let $f \in L^2(R)$. For $n \in Z$, $T_n : L^2(R) \to L^2(R)$ be given by $(T_n f)(x) = f(x-n)$ and $D : L^2(R) \to L^2(R)$ be given by $(Df)(x) = \sqrt{2}f(2x)$ operators T_n and D are called translation and dilation operator.

Definition 2. A function $\phi \in L^2(R)$ is called an orthonormal wavelet for $L^2(R)$ if $\{D^k T_n \phi : k, n \in Z\} = \{2^{k/2}\phi(2^{Kk} - n) : k, n \in Z\}$ is an orthonormal basis for $L^2(R)$.

Definition 3. A set of closed subspace $\{V_j : j \in Z\}$ of $L^2(R)$ is called a Multiresolution Analysis (MRA) if the following properties hold.

- $V_j \subseteq V_{j+1}$, for all $j \in Z$;
- $D(V_j) = D(V_{j+1})$, for all $j \in Z$;
- $\cup_{j\in Z} V_j = L^2(R)$, and $\cap_{j\in Z} V_j = 0$;
- There is a scaling function ϕ for V_0.

By a scaling function for V_0 we mean that there exists a function $\phi \in V_0$ such that $\{T_n\phi : n \in Z\}$ is an orthonormal basis for V_0. If we think of the core subspaces V_0 as a specified level of resolution then moving to amounts to Zooming in and increasing resolution by one level, on the other hand, V_{-1} represents one lower level of resolution, resulting from Zooming out. The first curve $h_0(t)$ also known as scaling function is defined as $h_0 = 1$ for $0 \le x < 1$ and 0 otherwise. The second curve h_1 is obtained after distributing the interval $[0, 1]$ in $[0, 0.5]$ and $[0.5, 1]$. Then, $h_1 = 1$ for $0 \le x < \frac{1}{2}$, -1 for $\frac{1}{2} \le x < 1$ and 0 otherwise. This is also called mother wavelet. All other subsequent curves are generated from $h_1(t)$. $h_2(t)$ is obtained from $h_1(t)$ with dilation. Other way, we can express Haar functions in a more compact form as

$$h_n(x) = h_1(2^j x - k),\ n = 2^j + k, \quad j \ge 0, \quad 0 < k \le 2^j \tag{2.1}$$

Having benefits of the Haar wavelet approach for its simplicity and sparse matrices of presentation, they are faster than others. Any function which is square integrable in the interval $[0, 1)$, can be expanded in a Haar series with an infinite number of terms as

$$u(x) = \sum_{i=0}^{\infty} \alpha_i h_i(x), \quad i = 2^j + k,\ j \ge 0, \quad 0 \le k \le 2^j, \quad x \in [0, 1) \tag{2.2}$$

where Haar coefficients $\alpha_i = 2^j \int_0^1 u(x)h_i(x)dx$ are determined in such a way that the integral square error

$$E = \int_0^1 [u(x) - \sum_{i=0}^{m-1} \alpha_i h_i(x)]^2, \quad m = 2^j, \quad j \in \{0\} \cup N \tag{2.3}$$

is minimized by applying the orthogonal relationship

$$\int_0^1 h_i(x)h_l(x)dx = 2^{-j}\delta_{il} = \begin{cases} 2^{-j}, & i = l = 2^j + k,\ j \ge 0, 0 \le k < 2^j; \\ 0, & i \ne l. \end{cases} \tag{2.4}$$

In general, for the function $u(x)$ to be smooth the series (2.1) contains an infinite number of terms. If $u(x)$ is a piecewise constant or may be approximated as piecewise constants, then the sum in equation (2.2) will be terminated after m terms, that is

$$u(x) = \sum_{i=0}^{m-1} \alpha_i h_i(x) \tag{2.5}$$

where $t \in [0, 1)$ and $\alpha_m = [\alpha_0, \alpha_1, \ldots, \alpha_{m-1}]^T$. Identifying the collocation points as $x_l = \frac{2l-1}{2m}$; $l = 1, 2, \ldots, m$, we have $h_m(x) = [h_0(x), \ldots, h_{m-1}(x)]^T$ and thus we obtain the haar functions as

$$h_0 = [1\ 1\ 1\ 1],\ h_1 = [1\ 1\ -1\ -1],\ h_2 = [1\ -1\ 0\ 0],\ h_3 = [0\ 0\ 1\ -1].$$

In other way the coefficients matrix $H_{il} = h_i(x_l)$ is introduced which is expanded into Haar series with coefficient matrix P as

$$\int_0^1 h_m(x)dx \cong P_{m\times m} h_m(x),\ t \in [0, 1). \tag{2.6}$$

where $m \times m$ square matrix P is called the operational matrix of integration and cam be expressed as

$$P_m = \frac{1}{2m} \begin{pmatrix} 2m\mathbf{P}_{m/2} & -\mathbf{H}_{m/2} \\ \mathbf{H}_{m/2}^{-1} & \mathbf{O}_{m/2} \end{pmatrix}$$

in particular, we get $P_{1\times 1} = [1/2]$. The other elements of the matrices H, P can be evaluated as

$$H_2 = \begin{pmatrix} 1 & 1 \\ 1 & -1 \end{pmatrix},\ P_2 = \frac{1}{4}\begin{pmatrix} 2 & -1 \\ 1 & 0 \end{pmatrix},\ H_4 = \begin{pmatrix} 1 & 1 & 1 & 1 \\ 1 & 1 & -1 & -1 \\ 1 & -1 & 0 & 0 \\ 0 & 0 & 1 & -1 \end{pmatrix}$$

$$P_4 = \frac{1}{16}\begin{pmatrix} 8 & -4 & -2 & -2 \\ 4 & 0 & -2 & 2 \\ 1 & 1 & 0 & 0 \\ 1 & -1 & 0 & 0 \end{pmatrix},\ H_8 = \begin{pmatrix} 1 & 1 & 1 & 1 & 1 & 1 & 1 & 1 \\ 1 & 1 & 1 & 1 & -1 & -1 & -1 & -1 \\ 1 & 1 & -1 & -1 & -1 & -1 & -1 & -1 \\ 0 & 0 & 0 & 0 & 1 & 1 & -1 & -1 \\ 1 & -1 & 0 & 0 & 0 & 0 & 0 & 0 \\ 0 & 0 & 1 & -1 & 0 & 0 & 0 & 0 \\ 0 & 0 & 1 & -1 & 0 & 0 & 0 & 0 \\ 0 & 0 & 0 & 0 & 0 & 0 & 1 & -1 \end{pmatrix}$$

$$P_8 = \frac{1}{64}\begin{pmatrix} 32 & -16 & -8 & -8 & -4 & -4 & -4 & -4 \\ 16 & 0 & -8 & 8 & -4 & -4 & 4 & 4 \\ 4 & 4 & 0 & 0 & -4 & 4 & 0 & 0 \\ 4 & 4 & 0 & 0 & -4 & 4 & 0 & 0 \\ 1 & 1 & 2 & 0 & 0 & 0 & 0 & 0 \\ 1 & 1 & -2 & 0 & 0 & 0 & 0 & 0 \\ 1 & -1 & 0 & 2 & 0 & 0 & 0 & 0 \\ 1 & -1 & 0 & -2 & 0 & 0 & 0 & 0 \end{pmatrix}$$

In the next section, we use these haar matrices to approximate the solution to the governing differential equation.

3. **Solution Procedure**

For the governing differential equation (1.1), $x \in [a, b]$, the interval is partitioned into $2M$ subintervals of equal length. Dividing the given interval into N equal parts of length $\Delta t = (0, 1]/N$. We use the approximation

$$\ddot{u}''(x,t) = \sum_{i=0}^{m-1} \alpha_i h_i(x), \tag{3.1}$$

where $h_i(x)$ are haar wavelet functions and α_i are wavelet coefficients, from (3.1), we have

$$u''(x,t) = (t-t_s)\sum_{i=0}^{m-1} \alpha_i h_i(x) + u''(x,t_s), \tag{3.2}$$

$$u'(x,t) = (t-t_s)\sum_{i=0}^{m-1} \alpha_i p_{i,1}(x) + u'(x,t_s) - u'(0,t_s) + u'(0,t), \tag{3.3}$$

$$\begin{aligned} u(x,t) &= (t-t_s)\sum_{i=0}^{m-1} \alpha_i p_{i,2}(x) + u(x,t_s) - u(0,t_s) \\ &\quad -x[u'(0,t_s) - u'(0,t)] + u(0,t), \end{aligned} \tag{3.4}$$

$$\dot{u}'(x,t) = \sum_{i=0}^{m-1} \alpha_i p_{i,1}(x) + \dot{u}'(0,t), \tag{3.5}$$

$$\dot{u}(x,t) = \sum_{i=0}^{m-1} \alpha_i p_{i,2}(x) + x\dot{u}'(0,t) + \dot{u}(0,t). \tag{3.6}$$

Using boundary conditions, we have

$$\begin{aligned} u(0,t) &= g_0(t),\ u(0,t_s) = g_0(t_s),\ \dot{u}(0,t_s) = g_0'(t_s), \\ u(0,t) &= g_0(t),\ \dot{u}(0,t) = g_0'(t),\ u(1,t) = g_1(t), \\ u(1,t_s) &= g_1(t_s),\ u(1,t_s) = g_1'(t_s),\ \dot{u}(1,t) = g_1'(t). \end{aligned} \tag{3.7}$$

Now, from (3.7), and taking $x = 1$,

$$g_1(t) = (t-t_s)\alpha_i p_{i,2}(1) + g_1(t_s) - g_0(t_s) - [u'(0,t_s) - u'(0,t)] + g_0(t),$$

$$u'(0,t_s) - u'(0,t) = -(t-t_s)\sum_{i=0}^{m-1}\alpha_i p_{i,2}(1) + g_1(t) - g_1(t_s) + g_0(t_s) - g_0(t). \tag{3.8}$$

From (3.6) we obtain

$$\dot{u}(1,t) = \sum_{i=0}^{m-1}\alpha_i p_{i,2}(1) + \dot{u}'(0,t) + \dot{u}(0,t). \tag{3.9}$$

Using the conditions (3.7)

$$\begin{aligned}\dot{u}'(0,t) &= -\sum_{i=0}^{m-1}\alpha_i p_{i,2}(1) - \dot{u}(0,t) - \dot{u}(1,t)\\ &= -\sum_{i=0}^{m-1}\alpha_i p_{i,2}(1) - g_0'(t) + g_1'(t). \end{aligned}\tag{3.10}$$

Substituting (3.8–3.10) in (3.2–3.4), replacing x by x_l , t by t_{s+1} and defining $(t_{s+1} - t_s) = \Delta t$, gives

$$u''(x_l,t_{s+1}) = \Delta t\sum_{i=0}^{m-1}\alpha_i h(x_l) + u''(x_l,t_s) \tag{3.11}$$

$$\begin{aligned}u'(x_l,t_{s+1}) &= \Delta t\sum_{i=0}^{m-1}\alpha_i p_{i,1}(x_l) - \Delta t\sum_{i=0}^{m-1}\alpha_i p_{i,2}(1)\\ &\quad + u(x_l,t_s) + g_1(t_{s+1}) - g_1(t_s) + g_0(t_s) - g_0(t_{s+1})\end{aligned}\tag{3.12}$$

$$\begin{aligned}u(x_l,t_{s+1}) &= \Delta t\sum_{i=0}^{m-1}\alpha_i p_{i,2}(x_l) + u(x_l,t_s) - x_l[\Delta t\sum_{i=0}^{m-1}\alpha_i p_{i,2}(1)\\ &\quad - g_1(t_{s+1}) + g_1(t_s) - g_0(t_s) + g_0(t_{s+1})] + g_0(t_{s+1}) - g_0(t_s)\end{aligned}\tag{3.13}$$

$$\dot{u}(x_l,t_{s+1}) = \sum_{i=0}^{m-1}\alpha_i p_{i,2}(x_l) - x_l[\sum_{i=0}^{m-1}\alpha_i p_{i,1}(1) + g_0'(t_{s+1}) - g_1'(t_{s+1})] + g_0'(t_{s+1})$$

(3.14)

where

$$p_{i,2}(1) = \begin{cases} 0.5, & \text{if } i = 1;\\ \frac{1}{4m^2}, & \text{if } i > 1.\end{cases}$$

Thus, for the governing advection-diffusion model (1.1) in hand, we have

$$\dot{u}(x_l,t_{s+1}) + \rho u'(x_l,t_{s+1}) - \varepsilon u''(x_l,t_{s+1}) = 0 \tag{3.15}$$

substituting (3.11)–(3.13)

$$\begin{aligned}&\sum_{i=0}^{m-1}\alpha_i p_{i,2}(x_l) - x_l\Big[\sum_{i=0}^{m-1}\alpha_i p_{i,1}(1) + g_0'(t_{s+1}) - g_1'(t_{s+1})] + g_0'(t_{s+1})\\ &+\rho\Big[\Delta t\sum_{i=0}^{m-1}\alpha_i p_{i,1}(x_l) - \Delta t\sum_{i=0}^{m-1}\alpha_i p_{i,2}(1) + u(x_l,t_s) + g_1(t_{s+1})\\ &-g_1(t_s) + g_0(t_s) - g_0(t_{s+1})\Big] - \varepsilon[\Delta t\sum_{i=0}^{m-1}\alpha_i h(x_l) + u''(x_l,t_s)\Big] = 0\end{aligned}\tag{3.16}$$

Finally, we get the system of equations for calculating the wavelet coefficients $\alpha_i s$.

$$\begin{aligned}\sum_{i=0}^{m-1}\alpha_i\Big[p_{i,2}(x_l)-x_l p_{i,1}(1)\rho\Delta t p_{i,1}(x_l)-\Delta t p_{i,2}(1)+\varepsilon\Delta t h_i(x_l)\Big]\\ =x_l\Big[g_0'(t_{s+1})-g_1'(t_{s+1})]-g_0'(t_{s+1})\\ -\rho\Big[u'(x_l,t_s)+g_1(t_{s+1})-g_1(t_s)+g_0(t_s)-g_0(t_{s+1})+\varepsilon u''(x_l,t_s)\Big]\end{aligned} \tag{3.17}$$

Taking into account the initial conditions, we start solving the system of equations for each time step with $t_{s+1}-t_s=\Delta t$ Experiments are carried out with some numerical examples listed below.

4. **Test Problems**

In this section, we present some numerical examples to demonstrate the effectiveness of proposed method of solution. Some numerical examples are described in this section. The first example is for a simple linear advection-diffusion process. The second and third examples demonstrate applications of time dependent Dirichlet boundary conditions. In the literature review, these examples have been studied widely by [17, 18]. An important non-dimensional parameter in numerical analysis is the Courant number $C_r=\rho\frac{\Delta t}{\Delta x}$. It is possible to show using a Fourier error analysis that the transport equation is stable for $C_r<1$. The Peclet number is another important non-dimensional term which compares the characteristic time for dispersion and diffusion given a length scale with the characteristic time for advection. In numerical analysis, one normally refers to a grid Peclet number $P_c=\rho\frac{\Delta x}{\varepsilon}$, where ρ is generally the velocity of water flow and the characteristic length scale is given by Δx. It compares the rate of advection ε to diffusion $\varepsilon/\Delta x$. More details regarding the effects of the Courant and Peclet numbers on the results can be found in [19]. In the present case, numerical results are computed by extracting collocation points for each level of resolution $J=2,3,4,5,6$. Generated points are taken to define the h_i and corresponding integrations are carried out. The index i is calculated by $i=m+k+1$ as explained in Section 2 where we have $h_1=1$ for $i=1$. Accuracy of the given approach is estimated by the error function

$$e_J=\frac{1}{2m}\|u(x,t)_{app}-u(x,t)_{ex}\| \tag{4.1}$$

Example 1.

Initially we begin with the simple example of linear advection-diffusion equation to demonstrate the working of scheme. For this, we consider the advection-diffusion problem in one dimension on a domain of unit length with the following boundary conditions

$$-\varepsilon u''+\rho u'=1,\ u(0)=u(1)=0. \tag{4.2}$$

Assuming a constant advection speed, ρ, and diffusivity $\varepsilon>0$. The onset of a boundary layer can be seen in Fig 1 corresponding to $\rho=1$ and several values of ε ($\varepsilon=0.01,0.1,1.0$). Simultaneously, solution profiles for the existing values of ε at a wider range can be seen along with the behavior of solution profile in three dimensional view.

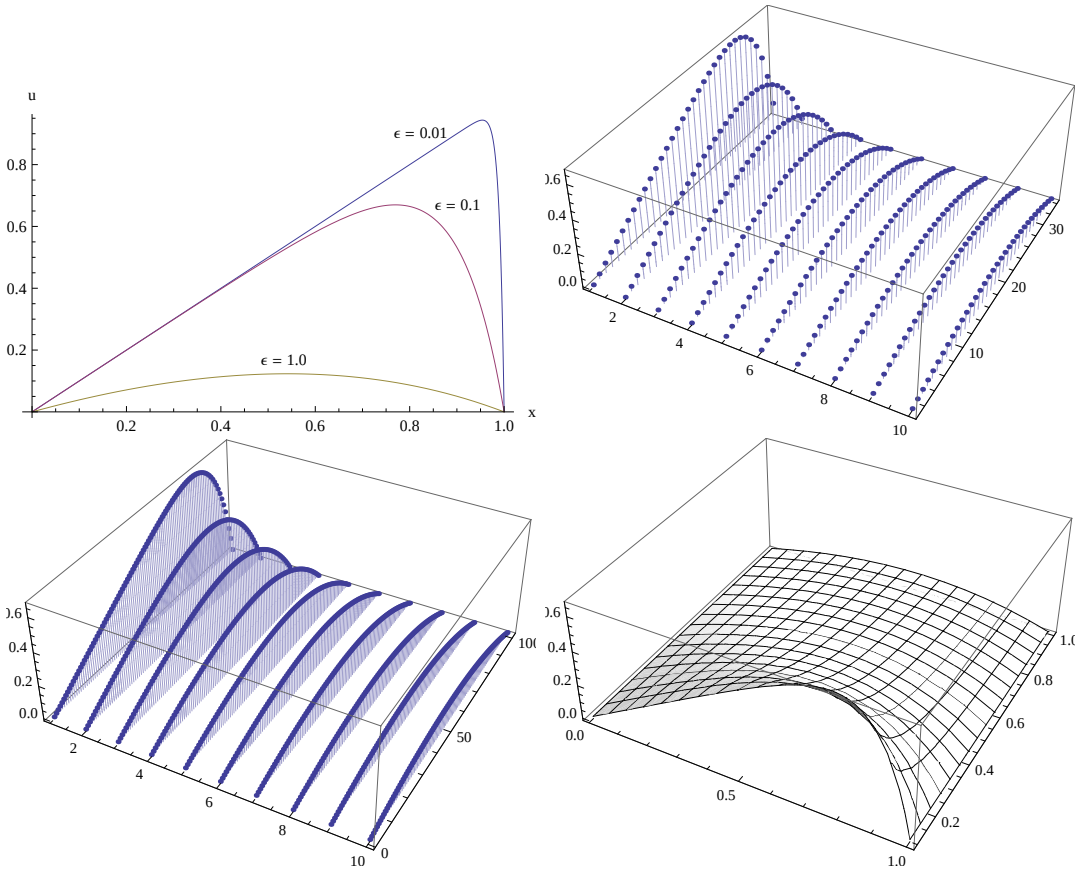

FIGURE 1. Results obtained for $\rho = 1.0, \varepsilon = 0.01, 0.1, 1.0$ for Experiment 1.

TABLE 1. Error estimation for Experiment 2 at different levels of resolution.

2M	e_J		
	$\Delta t = 0.001$	$\Delta t = 0.003$	$\Delta t = 0.005$
8	5.24E-3	3.28E-4	4.64E-5
16	3.13E-5	4.46E-3	5.34E-5
32	6.24E-6	5.34E-5	4.45E-3
64	4.43E-4	6.25E-4	6.55E-5
128	5.42E-3	4.11E-3	5.16E-5

Example 2.

In the second case, we have the one-dimensional advection-diffusion equation (1.1) in the region bounded by $0 \leq x \leq 1$, taking $\rho = 1.0$, $\varepsilon = 0.01$ with initial condition $f(x) = \exp\left(-\frac{(x+0.5)^2}{(0.00125)}\right)$ and boundary conditions $g_0 = \frac{0.025}{\sqrt{0.000625+0.02t}} \exp\left(-\frac{(0.5-t)^2}{(0.00125+0.04t)}\right)$,

$g_1 = \frac{0.025}{\sqrt{0.000625+0.02t}} \exp\left(-\frac{(1.5-t)^2}{(0.00125+0.04t)}\right)$. Figure 2 represents the concentration distribution at $t = 0.6, 0.7, 0.8, 0.9$ for $\rho = 1.0, \varepsilon = 0.01$. Varying time in the interval $0.6 \leq t \leq 0.9$ variation of solution profile can be observed sidewise. Physical behavior of the solution profile in 3D is also visible for this case. In all the results, a good agreement is observed between the solutions. In addition to this, Error analysis for the resolution level $J = 2, 3, 4, 5, 6$ is made in Table 1 taking step sizes $\Delta t = 0.001$, $\Delta t = 0.003$, $\Delta t = 0.005$ respectively.

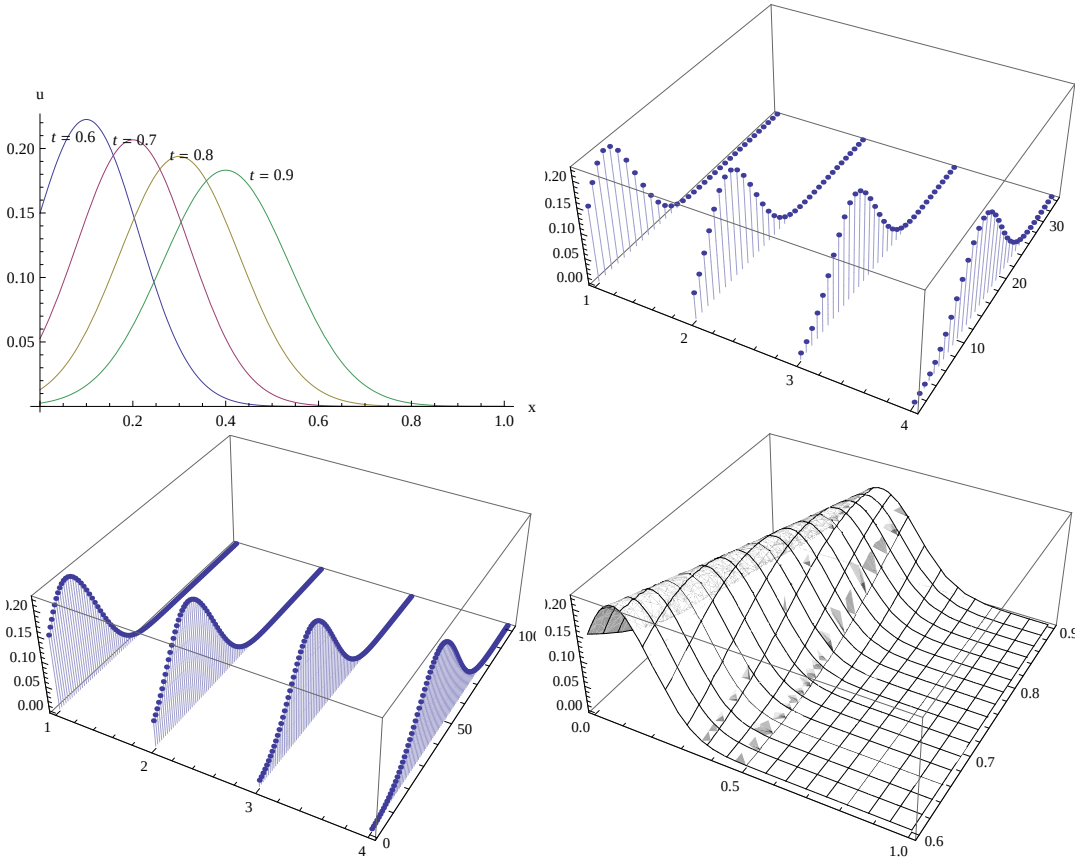

FIGURE 2. Results obtained for $\rho = 1.0, \varepsilon = 0.01$ at different times for Experiment 2.

Example 3.

In the third test case, we have initial and boundary conditions as $f(x) = 0$, $x > 0$ and $g_0(t) = 1.0$, $x = 0$ $g_1(t) = 0$, $x \to \infty$. Computations in this case are performed with different values of ρ, ε. Steepening effects of concentration profile can be seen with the change in time. In the first attempt, we have advection and diffusion coefficients ρ, ε as $\rho = 1.0$, $\varepsilon = 0.02$ respectively. Fig 3 draws attention for this case where solution profile is available at $t = 0, 1.0, 1.5, 2.0$ respectively. Impact of advection-diffusion process can be observed likewise in generalised interfaces. Next attempts are made for $\rho = 0.5, \varepsilon = 0.01$ and $\rho = 0.3, \varepsilon = 0.1$ respectively. Graphical results are neatly plotted in Figs. 4 and 5. In addition to this, error estimation for Experiment 3 at different levels of resolution can

TABLE 2. Error estimation for Experiment 3 at different levels of resolution.

2M	e_J		
	$\Delta t = 0.01$	$\Delta t = 0.001$	$\Delta t = 0.003$
8	4.33E-4	3.14E-3	4.22E-4
16	3.26E-3	4.54E-3	5.54E-5
32	7.44E-3	5.22E-3	4.33E-4
64	5.25E-5	6.81E-4	6.34E-5
128	5.22E-3	4.33E-3	5.43E-4

TABLE 3. Computed numerical data at $t = 0.7$ for three test cases.

2M	Experiment 1 $\varepsilon = 0.7$	Experiment 2 $\rho = 1.0, \varepsilon = 0.01$	Experiment3 $\rho = 0.5, \varepsilon = 0.01$
0.0313	0.01576042	0.07408752	0.9995043
0.0938	0.04758043	0.14053233	0.9944194
0.1563	0.07242575	0.19163535	0.9724752
0.2188	0.10212832	0.20225542	0.9094742
0.2813	0.12539452	0.16695834	0.7805394
0.3438	0.14290235	0.10299552	0.5871842
0.4063	0.15630122	0.04628211	0.3717254
0.4688	0.16820864	0.01649833	0.1919365
0.5313	0.17320332	0.00485521	0.0790671
0.5938	0.17282836	0.00103139	0.0255982
0.6563	0.16658125	0.00016774	0.0064473
0.7188	0.15391374	0.00002088	0.0012544
0.7813	0.13422536	1.99105×10^{-6}	0.0001876
0.8438	0.10686246	1.45314×10^{-7}	0.00002151
0.9063	0.07110525	8.11963×10^{-9}	1.8848×10^{-6}
0.9688	0.02617243	3.47348×10^{-10}	1.2597×10^{-7}

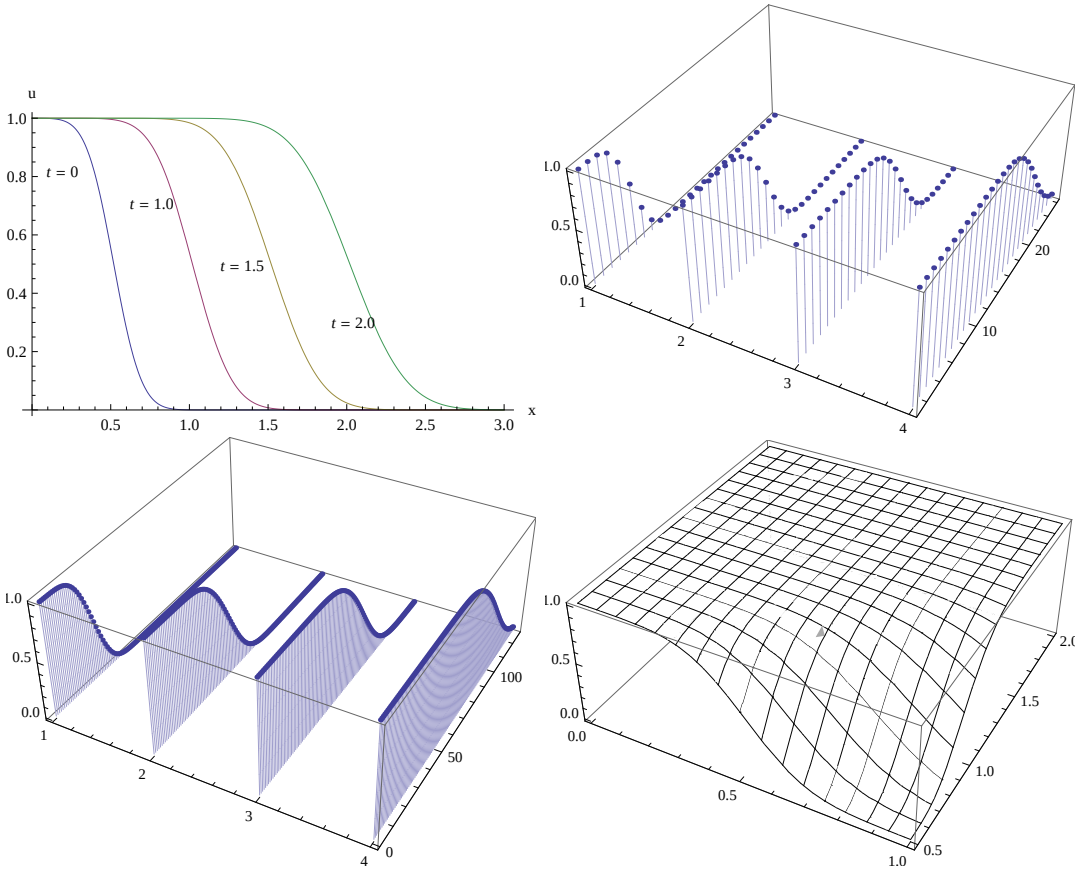

FIGURE 3. Results obtained for $\rho = 1.0, \varepsilon = 0.02$ at different times for Experiment 3.

be found in Table 2. For all the three cases, numerical results can be seen in Table 3 for resolution level $J = 3$.

5. **Conclusion**

In the present work, numerical technique based on Haar wavelets is presented to solve advection-diffusion model problem in a compact, clear and coherent way. Having benefits of the Haar wavelet approach for its simplicity and sparse matrices of presentation, given scheme is proved advantageous. Results are obtained for some test cases to check the working of proposed method. Numerical procedure presented here is well suited for a variety of mathematical models involving advection, diffusion phenomenon, heat transfer and others with feasible boundary/initial conditions.

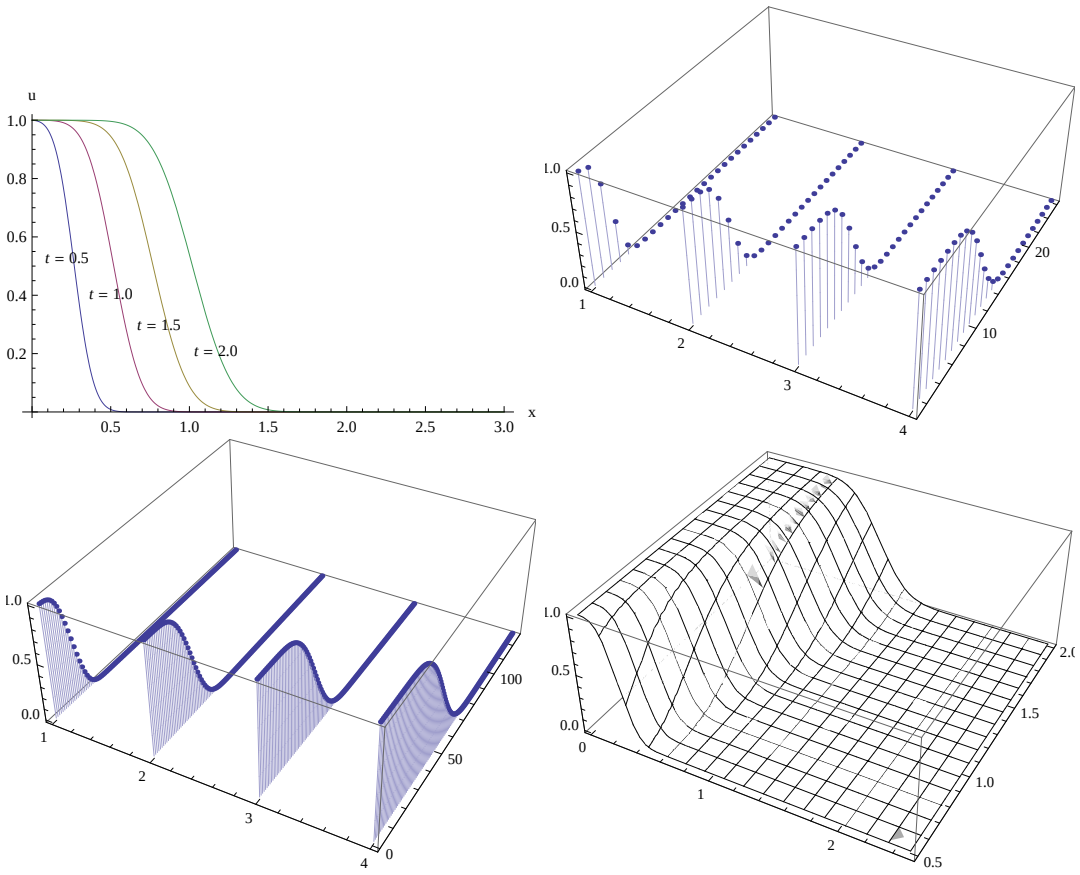

FIGURE 4. Results obtained for $\rho = 0.5, \varepsilon = 0.01$ at different times for Experiment 3.

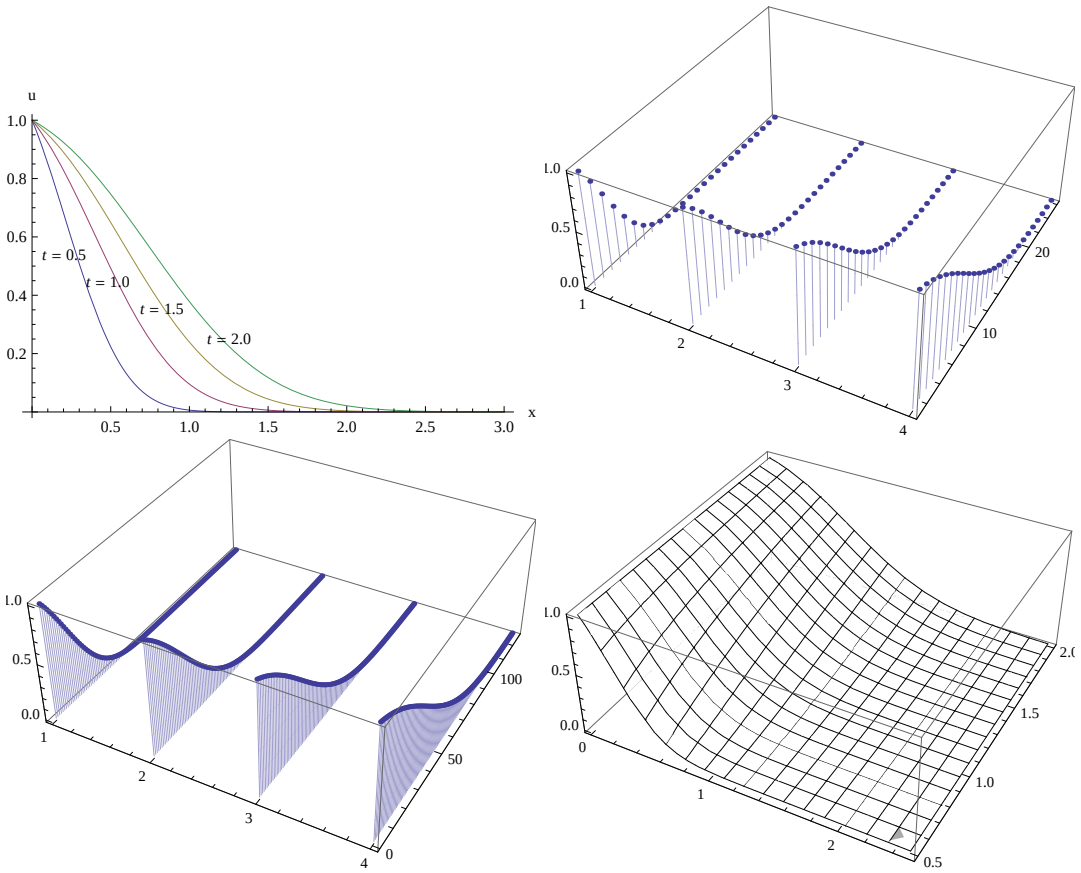

FIGURE 5. Results obtained for $\rho = 0.3, \varepsilon = 0.1$ at different times for Experiment 3.

REFERENCES

[1] Daubechies,I., *Ten Lectures on Wavelets*, SIAM, Philadelphia, PA, 1992.

[2] Mallat, S., *A wavelet Tour of Signal Processing*, Academic Press, New York, (1999).

[3] Daubechies, I., Orthonormal bases of compactly supported wavelets, *Comm. Pure Appl. Math.*, 909–996, 1988.

[4] Chen, C. F. and Hsiao, C. H., Haar wavelet method for solving lumped and distributedparameter systems, IEE Proc, number 144 in Control Theory Appl., 87–94, 1997.

[5] Hughes, T. J. R., Recent progress in the development and understanding of supg methods with special reference to the compressible euler and Navier-Stokes equations, *Int. J. Numer. Methods Engrg.* **7**: 1261–1275, 1987.

[6] Hughes, T. J. R., Franca, L. P. and Hulbert, G. M., A new finite element formulation for computational fluid dynamics: Viii. the Galerkin/least-squares method for advectivediffusive equations, *Comput. Methods Appl. Mech. Engrg.* **73**: 173–189, 1989.

[7] Chatwin, P. C. and Allen, C. M., Mathematical models of dispersion in rivers and estuaries, *Annual Review of Fluid Mechanics* **17**: 119–149, 1985.

[8] Morton, K.W., *Numerical solution of convection-diffusion equation*, Chapman & Hall, 1996.

[9] Johnson, C. and Saranen, J., Streamline diffusion methods for the incompressible euler and Navier-Stokes equations, *Math. Comput.* **47**: 1–18, 1986.

[10] Brooks, A. N. and Hughes, T. J. R., Streamline upwind/Petrov-Galerkin formulations for convection dominated flows with particular emphasis on the incompressible Navier-Stokes equations, *Comput. Methods Appl. Mech. Engrg.* **32**: 199–259, 1982.

[11] Codell, R. B., Key, K. T., and Whelan, G. A., *Collection of Mathematical Models for Dispersion in Surface Water and Groundwater*. NUREG 0868, U.S. Nuclear Regulatory Commission, Washington, DC, 1982.

[12] Perez-Guerrero, J. S., Pimentel, L. G., Skaggs, T. H., Van Genuchten, Analytical solution of the advection-diffusion transport equation using a change-of-variable and integral transform technique, *Int. J. Heat Mass Transfer* **52**: 3297–3304, 2009.

[13] Lepik, U., Solving integral and differential equations by the aid of non-uniform Haar wavelets, *Appl. Math. Comput.* **198**: 326–332, 2008.

[14] Lepik, U., Application of the Haar wavelet transform to solving integral and differential equations, *Proc Estonian Acad Sci Phys Math* **56**: 28–46, 2007.

[15] Manoj Kumar, Akhilesh Kumar Singh, Akanksha Srivastava, Various Newton-type iterative methods for solving nonlinear equations, *Journal of the Egyptian Mathematical Society* **21**: 334–339 2013.

[16] Mehdi Rashidi-Kouchi, A Numerical Solution of Chebyshev and Hermite Equations by Wavelet, *Applied Mathematical Sciences* **6**: 5349–5357, 2012.

[17] Dehghan, M., Weighted finite difference techniques for the one-dimensional advection-diffusion equation, *Appl. Math. Comput.* **147**: 307–319, 2004.

[18] Kadalbajoo, M. K. and Arora, P., Space-time Galerkin least-squares method for the one-dimensional advection-diffusion equation, *Int. J. Comput. Math.* **87**: 103–118, 2010.

[19] C. I. Steefel and K. T. B. MacQuarrie, Approaches to modeling reactive transport in porous media. In Reactive Transport in Porous Media (Lichtner PC, Steefel CI, Oelkers EH eds.), *Reviews in Mineralogy* **34**, 83–125, 1996.